



OPEN

METTL3-mediated m6A modification of LINC00857 enhances stemness and metastasis of ovarian cancer cells by activating the YAP-TEAD pathway

Xueke Lin^{1,2}, Yiting Hong², Shengjun You², Ping Li², Yuchun Lv², Jinyang Zheng³ & Pengming Sun^{1,4,5}✉

This study was designed to illustrate the mechanism underlying the up-regulation of LINC00857 expression and to identify novel molecular targets for the treatment of ovarian cancer (OC). The LINC00857 and methyltransferase-like 3 (METTL3) expression levels were observed in clinical OC tissues and cells, and their correlation within tissues was analyzed. To further explore the relationship between LINC00857 and METTL3, a combined transfection of pcDNA3.1-LINC00857 and METTL3 siRNA was performed. Subsequently, cell invasion, viability, migration, and sphere-forming capabilities were assessed using Transwell, Cell Counting Kit-8, scratch and sphere-formation assays. Furthermore, western blot analysis was conducted to determine the expression of proteins related to cancer cell stemness and the yes-associated protein (YAP) pathway. The relationship between LINC00857 and METTL3 was verified using the MeRIP-qPCR kit, RNA pull-down assay and RNA stability assay. Both LINC00857 and METTL3 demonstrated high expression levels in OC cells and tissues, with a positive correlation observed in clinical tissues. When knocking down the LINC00857 expression level, the invasion, migration, proliferation, and sphere-forming capabilities of cells were all notably reduced. Knocking down LINC00857 expression also markedly decreased the activity of the YAP pathway and the expression of proteins related to cancer cell stemness. Overexpression of LINC00857 yielded opposite effects. When knocking down METTL3, the stability of LINC00857 and the modification level of N6-methyladenosine were remarkably decreased. Moreover, there was interaction between METTL3 and LINC00857. METTL3-mediated N6-methyladenosine modification of LINC00857 enhanced metastasis and stemness of OC cells via activating the YAP-TEAD domain transcription factor pathway.

Keywords Ovarian cancer, Cancer stemness, LncRNA LINC00857, METTL3, M6A modification, YAP-TEAD

Abbreviations

OC	ovarian cancer
YAP	yes-associated protein
CCK-8	Cell Counting Kit-8
SOX2	SRY-box transcription factor 2
Oct4	octamer-binding transcription factor 4

¹College of Clinical Medicine for Obstetrics & Gynecology and Pediatrics, Fujian Medical University, Fuzhou 350001, Fujian, China. ²Department of Obstetrics and Gynecology, Quanzhou First Hospital Affiliated to Fujian Medical University, Quanzhou 362000, Fujian, China. ³Department of Pathology, Quanzhou First Hospital Affiliated to Fujian Medical University, Quanzhou 362000, Fujian, China. ⁴Laboratory of Gynecologic Oncology, College of Clinical Medicine for Obstetrics & Gynecology and Pediatrics, Fujian Maternity and Child Health Hospital, Fujian Medical University, Fuzhou 350001, Fujian, China. ⁵Fujian Clinical Research Center for Gynecological Oncology, Fujian Maternity and Child Health Hospital (Fujian Obstetrics and Gynecology Hospital), Fuzhou 350001, Fujian, China. ✉email: fmsun1975@fjmu.edu.cn

NANOG	Nanog homeobox
p-YAP1	phosphorylated-YAP1
LATS1	large tumor suppressor 1
p-LATS1	phosphorylated-LATS1
TEAD	TEA domain transcription factor
m6A	N6-methyladenosine
METTL3	methyltransferase-like 3
FBS	fetal bovine serum
EGF	epidermal growth factor

As changes in lifestyle and environmental conditions persist, the global incidence of cancer continues to rise, with ovarian cancer (OC) standing as one of the most lethal gynecological malignancies¹. In 2022, over 206,839 patients succumbed to OC², and the five-year survival rate is dismal 47.4%³. The high mortality rate of OC is primarily attributed to its asymptomatic onset, non-specific symptoms, and high invasiveness, which result in most patients being diagnosed at advanced stage⁴. Advancements in surgery, chemotherapy, and targeted therapies have led to improved short-term outcomes. However, the prognosis still remains poor due to high recurrence rates and chemoresistance, particularly to platinum-based therapies, which are considered the standard of care⁵. These clinical challenges underscore the urgent need to elucidate the molecular mechanisms underlying OC progression, drug resistance, and recurrence to develop novel and effective therapeutic strategies.

Long non-coding RNAs (lncRNAs) have emerged as critical regulators of cancer progression, influencing tumor growth, metastasis, and treatment resistance⁶. Among them, lncRNA LINC00857 has been identified as an oncogenic factor in multiple cancers. Silencing LINC00857 suppresses cell proliferation in colorectal and pancreatic cancers^{7,8}, and its up-regulation correlates with poor prognosis in gastric cancer⁹. In OC, LINC00857 is significantly overexpressed, and its knockdown suppresses tumor cell glycolysis, migration, invasion, proliferation, and promotes apoptosis¹⁰. Importantly, accumulating evidence suggests that cancer stemness, a key feature regulated by lncRNAs, plays a central role in chemoresistance and tumor relapse¹¹. Given its consistent oncogenic role across multiple cancer types and its marked upregulation in OC, LINC00857 represents a compelling candidate for mechanistic investigation, and clarifying its upstream regulation may reveal novel biomarkers and therapeutic targets to improve outcomes in OC.

Recent studies have revealed that N6-methyladenosine (m6A) modification plays a pivotal role in regulating lncRNA stability, localization, and function¹². It has been shown that m6A-modified lncRNAs contribute to cancer progression in several tumor types^{13,14}. Notably, Meng et al.¹⁵ demonstrated that m6A modification enhanced the stability of LINC00857, thereby promoting pancreatic cancer tumorigenesis. Because m6A modification is a key determinant of RNA stability, we speculated that methyltransferase-like 3 (METTL3), a core m6A methyltransferase previously identified as an oncogenic regulator in multiple cancers including OC^[16, 17], may act as a critical upstream regulator of LINC00857. Therefore, we hypothesize that METTL3-mediated m6A modification stabilizes LINC00857, thereby driving OC stemness, metastasis, and possibly chemoresistance via downstream signaling pathways.

To address this hypothesis, we conducted a series of in vitro experiments to explore the connections among METTL3, LINC00857, and OC progression, particularly their involvement in yes-associated protein (YAP)-TEA domain transcription factor (TEAD) pathway activation. Our findings aim to provide mechanistic insights into OC pathogenesis and identify potential molecular targets to overcome treatment resistance and recurrence, thereby improving patient outcomes.

Materials and methods

Collection of clinical tissues

Ethical approval for this study was obtained in advance from the Ethics Committee of Quanzhou First Hospital Affiliated to Fujian Medical University. All patients involved provided informed consent and volunteered to take part in this study. The study was conducted in accordance with the Declaration of Helsinki. The tumor tissues (OC group) and adjacent histologically normal tissues (Adjacent tissue group) were collected from OC patients receiving tumor resection surgery or pathological examination in our hospital. The inclusion criteria were as follows: (1) OC confirmed by histologic diagnosis; (2) occurrence of only one primary malignant tumor; (3) no evidence of lymph node metastasis; and (4) no chemotherapy administered within at least one month prior to surgery. Patients were excluded if they met any of the following: (1) concurrent multiple tumors and (2) the presence of other severe systemic diseases or complications.

Cell culture and transfection

Human normal epithelial ovarian cells (IOSE80) were purchased from Cas9X™ (TCH-C402, China). OC cells (OVCAR8) were provided by Procell Life Science&Technology Co., Ltd (CL-0178, China). All cells were cultured in a Roswell Park Memorial Institute 1640 Medium with 1% penicillin-streptomycin and 10% fetal bovine serum (FBS), and maintained at 37 °C with 95% air and 5% CO₂.

OVCAR8 cells were transfected with LINC00857 siRNA (GAGTGTGCACATATGTGTAATTATT) (si-LINC00857 group), control negative siRNA (GAGACGTATACGTGTTAATTGTATT) (si-NC group), negative pcDNA3.1 (Vector group), and pcDNA3.1-LINC00857 (OE-LINC00857 group), respectively, using ExFect Transfection Reagent (T101-01, Vazyme, China). Negative siRNA (CAGCTAGGATCTCGAATTAAAGAT A) (si-NC group) and METTL3 siRNA (CAGGAGATCCTAGAGCTATTAATA) (si-METTL3 group) were transfected into OVCAR8 cells. To observe the relationship between METTL3 and LINC00857, METTL3 siRNA and pcDNA3.1-LINC00857 were simultaneously transfected into OVCAR8 cells (si-METTL3 + OE-LINC00857 group).

CCK-8 assay

Cells (5×10^3 cells/well) were seeded in a 96-well plate (Corning, USA) and subjected to transfection. After 48 h, cell viability was assessed using the Cell Counting Kit-8 (CCK-8, HY-K0301, MCE, USA) according to the manufacturer's protocol. Specifically, each well was supplemented with 10 μ L of CCK-8 reagent, followed by four-hour incubation in an incubator at 37 °C. Then, the absorbance at 450 nm was recorded using a Multiskan™ FC microplate reader (1410101, ThermoFisher, USA) to calculate cell viability.

Transwell assay

To measure cell invasion, the upper chamber of a Transwell insert was pre-coated with Matrigel (50 mg/mL, BD Biosciences, USA) and incubated at 37 °C for 2 h. Forty-eight hours post-transfection, OVCAR8 cells (5×10^4 cells/well) suspended in the serum-free medium were seeded into the upper chamber, while the lower chamber was filled with a complete medium containing 10% FBS as a chemoattractant. Upon 48 h of incubation, non-invasive cells on the upper membrane surface were carefully removed using a cotton swab. The invasive cells on the lower surface were fixed with methanol, stained with 0.1% crystal violet, and counted under a microscope.

Scratch assay

OVCAR8 cells (5×10^5 cells/well) were introduced in a 6-well plate and cultured to 60–80% confluence. Following 48 h of transfection, a sterile pipette tip was utilized to create a uniform scratch. The cells were subsequently washed with PBS to remove debris, followed by the addition of a fresh medium. Lastly, a microscope was utilized to capture images of the wound area at 0 and 24 h, and ImageJ software was exploited for the quantification of the wound closure.

Sphere-formation assay

Following 48 h of transfection, OVCAR8 cells were harvested and a single cell suspension was prepared. The cells (1×10^3 cells/well) were seeded into an ultra-low attachment 6-well plate using a Roswell Park Memorial Institute (RPMI) 1640 Medium containing B27, 20 ng/mL basic fibroblast growth factor, and 20 ng/mL epidermal growth factor (EGF). Upon 10 days of incubation in a cell incubator, sphere formation was observed and photographed using a microscope.

qRT-PCR

The cell RNA extraction kit (abs60368, Absin, China) was carried out for the extraction of total RNA from transfected cells. Simultaneously, tissue RNA was purified in accordance with the tissue RNA extraction kit (abs60284, Absin, China). Dropnone (ThermoFisher, USA) was then adopted for the detection of the concentration of RNA. Subsequently, 1 μ g of total RNA was reverse-transcribed into cDNA with the GoScript™ Reverse Transcription System (A2790, Promega, USA). Finally, the qPCR reaction system, including quantitative primers, cDNA, and the GoTaq® Enviro qPCR System (AM2000, Promega, USA), was assembled and analyzed on the LightCycler96 instrument (Roche, USA). The gene expression levels were counted using a $2^{-\Delta\Delta CT}$ method with GAPDH as the internal reference (Table 1).

Western blot

First, transfected cells were lysed completely using the radioimmunoprecipitation assay (RIPA) lysate. After collecting the resulting supernatants, a bicinchoninic acid kit was employed for the determination of the protein concentration. Upon separation by 10% sodium dodecyl sulfate-polyacrylamide gel electrophoresis, 20 μ g protein was transferred onto polyvinylidene fluoride membranes (Bio-Rad, USA). The membranes were then blocked with 5% skim milk at ambient temperature for 2 h. Subsequently, the incubation of the membranes was conducted overnight using the following primary antibodies at 4 °C: YAP1 (ab205270, Abcam, 1:1000), SRY-box transcription factor 2 (SOX2, ab92494, Abcam, 1:1000), octamer-binding transcription factor 4 (Oct4, ab200834, Abcam, 1:1000), Nanog homeobox (NANOG, ab109250, Abcam, 1:1000), phosphorylated-YAP1 (p-YAP1, ab254343, Abcam, 1:1000), large tumor suppressor 1 (LATS1, ab243656, Abcam, 1:1000), phosphorylated-LATS1 (p-LATS1, ab305029, Abcam, 1:1000), TEAD4 (ab308621, Abcam, 1:1000), METTL3 (ab195352, Abcam, 1:1000), and GAPDH (ab8245, Abcam, 1:1000). Next, the membranes were incubated for 2 h at ambient temperature with horseradish peroxidase (HRP)-labeled secondary antibodies (Goat Anti-Mouse IgG H&L-HRP, ab205719, Abcam, 1:5000; Goat Anti-Rabbit IgG H&L-HRP, ab6721, Abcam, 1:5000). Then, the protein bands were visualized using the enhanced chemiluminescence substrate (BL523A, Biosharp, China) in the ChemiDoc™ XRS imaging system (Biored, USA). The gray scale of the protein bands was scanned by ImageJ, with GAPDH serving as the internal reference for normalizing the target protein expression.

Gene name	Sequences (5' to 3')
LINC00857	F: CCCCTGCTTCATTGTTCC
	R: AGCTTGCTCTTCTGGTACT
METTL3	F: CTATCTCTGGCACTCGAAGA
	R: GCTTGAACCGTGCAACCACATC
GAPDH	F: GTCTCCTCTGACTTCAACAGCG
	R: ACCACCCCTGTTGCTGTAGCCAA

Table 1. qRT-PCR primers.

Immunohistochemistry

Tissues were sectioned into 5 μ m thick slices using an ultramicrotome (EM UC7, Leica, Germany) and mounted on slides. The sections were incubated in 0.4% Triton X-100 (P0096, Beyotime, China) for 15 min, followed by blocking in 1% sheep serum (SL038, Solarbio, China) for 15 min. They were then incubated with the primary antibody YAP1 (ab205270, Abcam, 1:500) at ambient temperature for 2 h, and subsequently with HRP-labeled secondary antibody (Goat Anti-Rabbit IgG H&L-HRP, ab6721, Abcam, 1:5000) for 1 h at room temperature. Next, the sections were immersed in enhanced chemiluminescence substrates (BL523A, Biosharp, China) for 15 min and washed. Finally, the protein expression was observed and recorded under a microscope.

m6A enrichment detection

After completing the previously mentioned RNA extraction steps, the RNA was purified, and the concentration was detected using Dropnone (ThermoFisher, USA). Next, equal amounts of RNA and m6A antibody (ab151230, Abcam, UK) were mixed, followed by 4-hour incubation at 4°C. Subsequently, Protein A/G magnetic beads (10002D, ThermoFisher, USA) were added to the mixture, which was then rotated at 4 °C for 1 h using a Revolver™ Mixer (Cygen, China). Afterward, the magnetic beads were adsorbed using DynaMag™-2 Magnet (12321D, ThermoFisher, USA). After the residual liquid was removed, 200 μ L washing buffer was added, and the mixture was gently pipetted to ensure uniform distribution. Following this, the mixture was incubated at 4°C for 5 min. Finally, DynaMag™-2 Magnet was used again to absorb the magnetic beads and qRT-PCR was utilized to collect the liquid to observe the content of LINC00857.

RNA pull-down assay

Normally cultured OVCAR8 cells were collected in a 1.5 Eppendorf tube and added with radioimmunoprecipitation assay lysate. After achieving complete cell lysis, the debris was removed. Following the instructions of the RNA pull-down kit (Bes5102, BersinBio, China), 2 μ g of biotin-labeled LINC00857 (Sangon biotech, China) was added to the cell lysate and incubated in a Revolver™ Mixer (Cygen, China) for 30 min at 30 °C. Subsequently, the mixture was incubated with streptavidin agarose in the Revolver™ Mixer (Cygen, China) at ambient temperature for 60 min. After adding the precipitate to the protein elution buffer, the protein was extracted and western blot was conducted in accordance with the aforementioned steps to observe the expression of METTL3. IgG was used as a negative control RNA probe.

RNA stability assay

Transfected OVCAR8 cells were exposed to 10 μ g/mL actinomycin D (HY-17559, MCE, USA) to inhibit transcription. RNA was extracted at 0, 2, 4, and 6 h post-treatment, and LINC00857 levels were observed using qRT-PCR. Next, RNA stability was assessed by comparing the decay rates of LINC00857 between different experimental groups.

Statistical analysis

All data were analyzed using GraphPad Prism 8.0 software and presented as mean \pm standard deviation (SD). An unpaired t-test was utilized to evaluate the differences between two groups, while a one-way analysis of variance was conducted for the assessment of differences among multiple groups. Statistical significance was defined as $P < 0.05$. Each experiment was performed at least three times independently.

Results

LINC00857 enhances the invasion, migration, proliferation, and stemness of ovarian cancer cell OVCAR8

LINC00857 expression in clinical tissues and cell lines was analyzed first to determine its relevance to OC progression. The results of qRT-PCR revealed that LINC00857 expression was significantly up-regulated in OC tissues compared to adjacent normal tissues (Fig. 1A) and in OVCAR8 cells compared to normal epithelial ovarian cells (IOSE80) (Fig. 1B) ($p < 0.01$).

Given the previous evidence that high LINC00857 expression promotes OC progression¹⁶, we knocked down or overexpressed the LINC00857 level in OVCAR8 cells. The qRT-PCR outcomes confirmed successful knockdown and overexpression of LINC00857 ($p < 0.01$) (Fig. 2A). According to the results of CCK-8, Transwell, scratch wound healing, and sphere-formation assays, knockdown of LINC00857 significantly inhibited cell viability, invasion, migration, and sphere-forming capabilities ($p < 0.01$). Conversely, overexpression of LINC00857 promoted these malignant behaviors ($p < 0.05$) (Figs. 2B–E).

To further assess the relationship between LINC00857 and cancer stemness, western blot analysis was conducted to examine the expression of stemness-related proteins. The examination results disclosed that knocking down LINC00857 considerably down-regulated the levels of SOX2, NANOG, and Oct4, while overexpression of LINC00857 significantly increased these levels ($p < 0.01$) (Fig. 2F–G). Collectively, these findings indicated that LINC00857 promoted OC progression by enhancing cell invasion, migration, proliferation, and stemness.

LINC00857 participates in YAP1 activation

Given the emerging role of LINC00857 in oncogenic pathways, we explored its relationship with the YAP1 signaling pathway, a critical regulator of tumor growth and stemness¹⁰. Using The Cancer Genome Atlas (TCGA) database, we identified a significant positive correlation between LINC00857 and YAP1 expression in OC ($p = 6.8e-09$) (Fig. 3A).

To validate this observation, we first detected YAP1 protein expression in OC tissues and OVCAR8 cells. YAP1 expression was remarkably elevated in OC tissues compared to adjacent tissues and in OVCAR8 cells compared to IOSE80 cells ($p < 0.01$) (Figs. 3B–C). Functional assays further demonstrated that knocking down

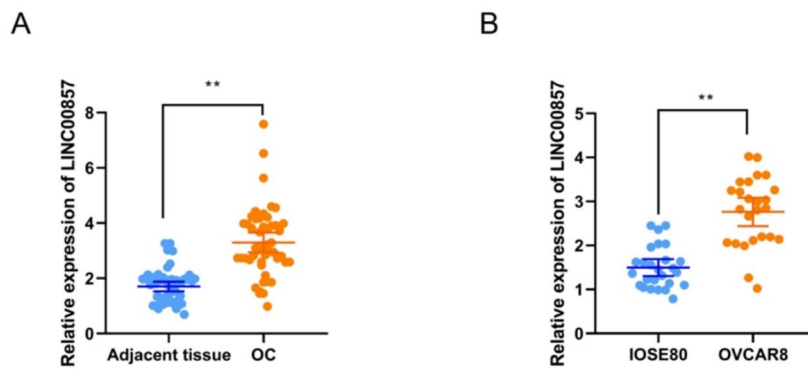


Fig. 1. Overexpression of lncRNA LINC00857 in ovarian cancer cells and tissues. (A) Relative expression levels of LINC00857 in OC tissues compared to adjacent normal tissues using qRT-PCR ($n=50$). (B) Relative expression levels of LINC00857 in OC cell line OVCAR8 compared to normal ovarian epithelial cell line IOSE80 using qRT-PCR ($n=25$). Data were presented as mean \pm SD; ** $p < 0.01$; statistical significance was determined using unpaired Student's t-test. OC, ovarian cancer.

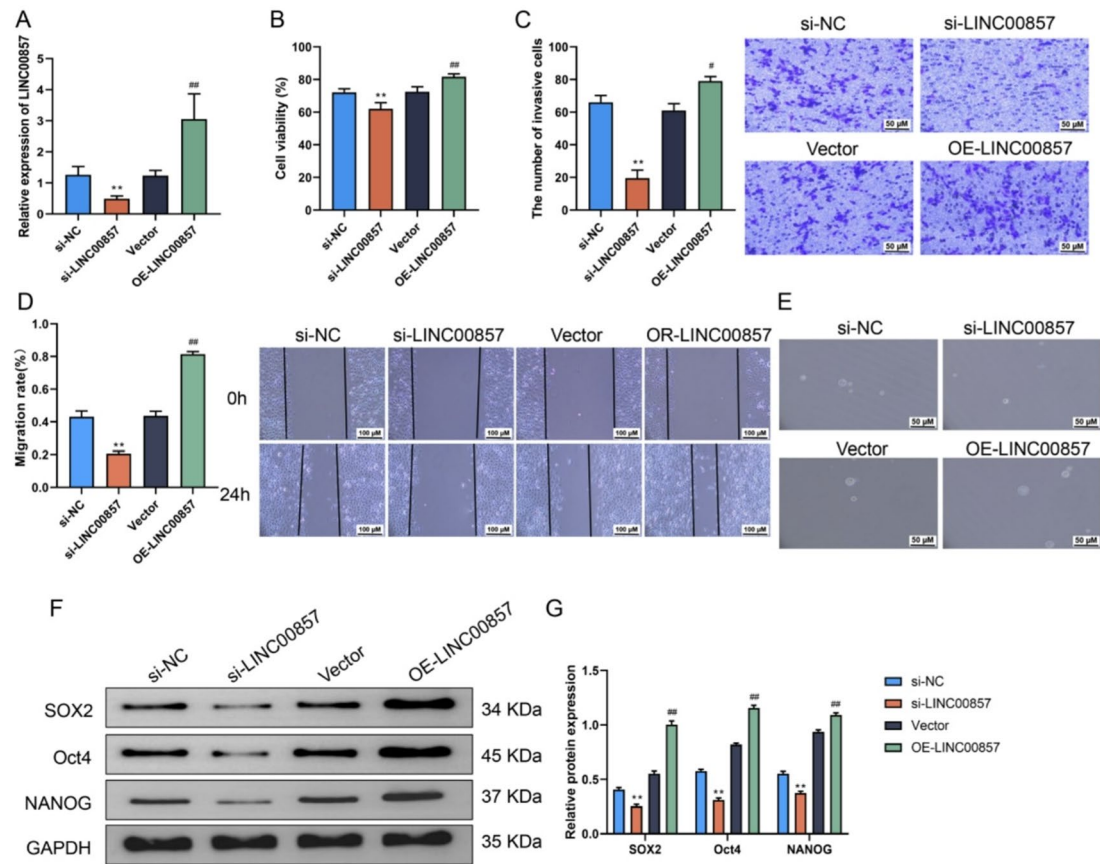


Fig. 2. LINC00857 enhances the invasion, migration, proliferation, and stemness of ovarian cancer cell OVCAR8. (A) qRT-PCR analysis of LINC00857 expression levels in OVCAR8 cells transfected with si-NC, si-LINC00857, the vector group, or a LINC00857 overexpression plasmid. (B) Cell viability was assessed using CCK-8 assay. (C) Cell invasion was evaluated using Transwell assay (scale bar = 50 μ m). (D) Cell migration was measured using scratch assay (scale bar = 100 μ m). (E) Representative images of sphere-formation assay showing the sphere-forming capacity of OVCAR8 cells in each group (scale bar = 50 μ m). (F-G) The protein levels of SOX2, NANOG, and Oct4 in OVCAR8 cells. Data were presented as mean \pm SD ($n=3 \sim 5$); ** $p < 0.01$ vs. si-NC; ## $p < 0.01$ vs. Vector; statistical analysis was performed using one-way ANOVA followed by Tukey's post hoc test. CCK-8, Cell Counting Kit-8; SOX2, SRY-box transcription factor 2; NANOG, Nanog homeobox; Oct4, octamer-binding transcription factor 4.

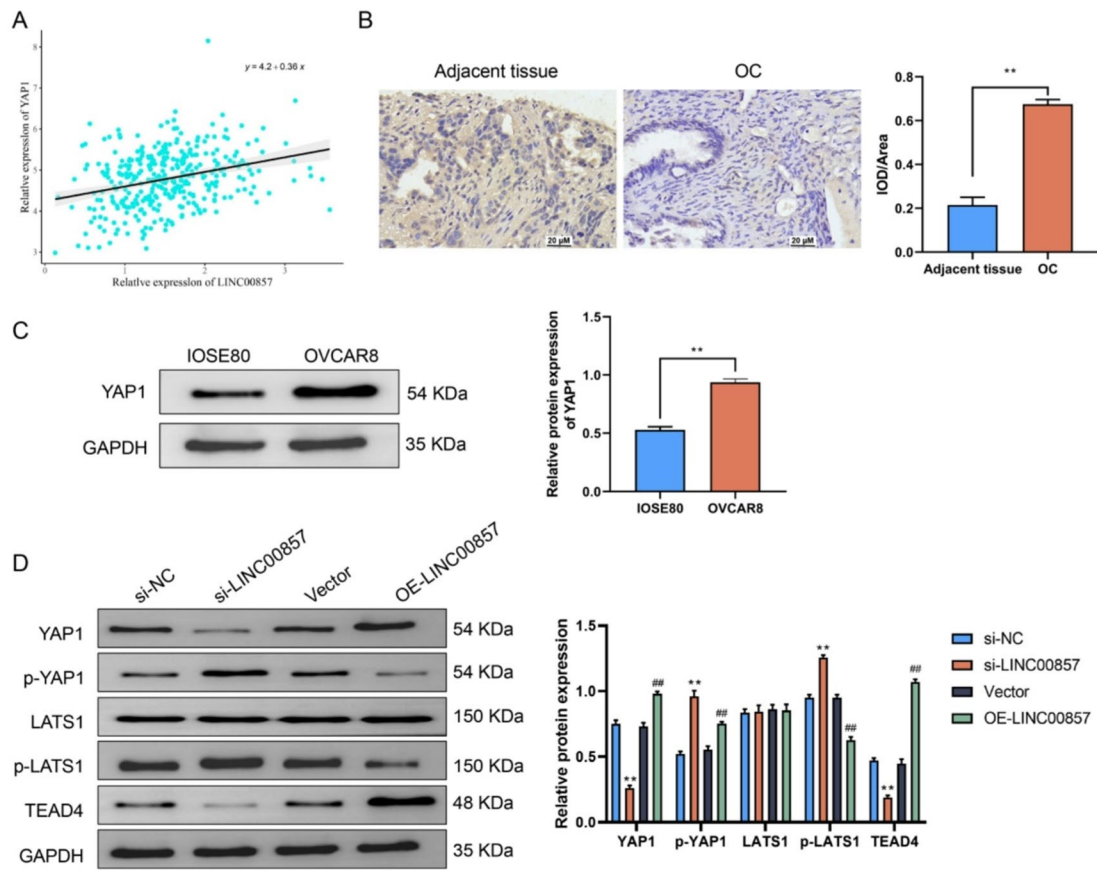


Fig. 3. LINC00857 participates in the activation of YAP1. **(A)** Correlation analysis between LINC00857 and YAP1 expression based on TCGA database ($n = 353$). **(B)** Immunohistochemistry analysis of YAP1 levels in OC tissues compared to adjacent tissues (scale bar = 20 μ m); ** $p < 0.01$. **(C)** Western blot analysis of YAP1 protein expression levels in IOSE80 and OVCAR8 cells; ** $p < 0.01$. **(D)** Western blot analysis of YAP1, p-YAP1, LATS1, p-LATS1, and TEAD4 protein levels in OVCAR8 cells across groups. Data were presented as mean \pm SD ($n = 3$); ** $p < 0.01$ vs. si-NC; ## $p < 0.01$ vs. Vector; statistical analysis was performed using unpaired two-tailed Student's t-test (for two-group comparisons) or one-way ANOVA followed by Tukey's post hoc test (for multiple comparisons). YAP1, yes-associated protein 1; TCGA, The Cancer Genome Atlas; OC, ovarian cancer; p-YAP1, phosphorylated-YAP1; LATS1, large tumor suppressor 1; p-LATS1, phosphorylated-LATS1; TEAD4, TEA domain transcription factor 4.

LINC00857 considerably reduced the levels of YAP1 and TEAD4, while increasing the phosphorylation levels of YAP1 (p-YAP1) and LATS1 (p-LATS1), indicating inactivation of the YAP1 pathway. Conversely, overexpression of LINC00857 enhanced TEAD4 and YAP1 expression and decreased p-LATS1 and p-YAP1 levels ($p < 0.01$) (Fig. 3D). These results demonstrated that LINC00857 could significantly activate the YAP1 pathway.

METTL3 highly expresses in ovarian cancer cells and promotes the LINC00857 expression by m6A modification

To elucidate the mechanisms underlying LINC00857 up-regulation in OC, we investigated the role of m6A modification, a key regulator of RNA stability. Notably, METTL3, a primary m6A methyltransferase, has been implicated in multiple cancers¹⁷. As shown in Fig. 4, we observed that METTL3 expression was significantly up-regulated in OC tissues compared to adjacent normal tissues (Fig. 4A), and its expression positively correlated with LINC00857 levels (Fig. 4B) ($p < 0.01$). Similarly, METTL3 expression and LINC00857 m6A enrichment were significantly higher in OVCAR8 cells compared to IOSE80 cells ($p < 0.01$) (Fig. 4C–D).

To confirm METTL3's role in stabilizing LINC00857, METTL3 was knocked down in OVCAR8 cells. The analysis outcomes of qRT-PCR and western blot confirmed successful knockdown of METTL3 at both mRNA and protein levels ($p < 0.01$) (Fig. 4E–F). Notably, knockdown of METTL3 led to a significant decrease in LINC00857 expression (Fig. 4G) and its m6A enrichment (Fig. 4H) ($p < 0.01$). Using RNA pull-down and RNA stability assays, we identified a direct interaction between LINC00857 and METTL3, with METTL3 shown to enhance LINC00857 stability ($p < 0.01$) (Fig. 4I–J).

The results above illustrated that METTL3 up-regulation in OC promoted LINC00857 expression through m6A modification, contributing to its increased stability.

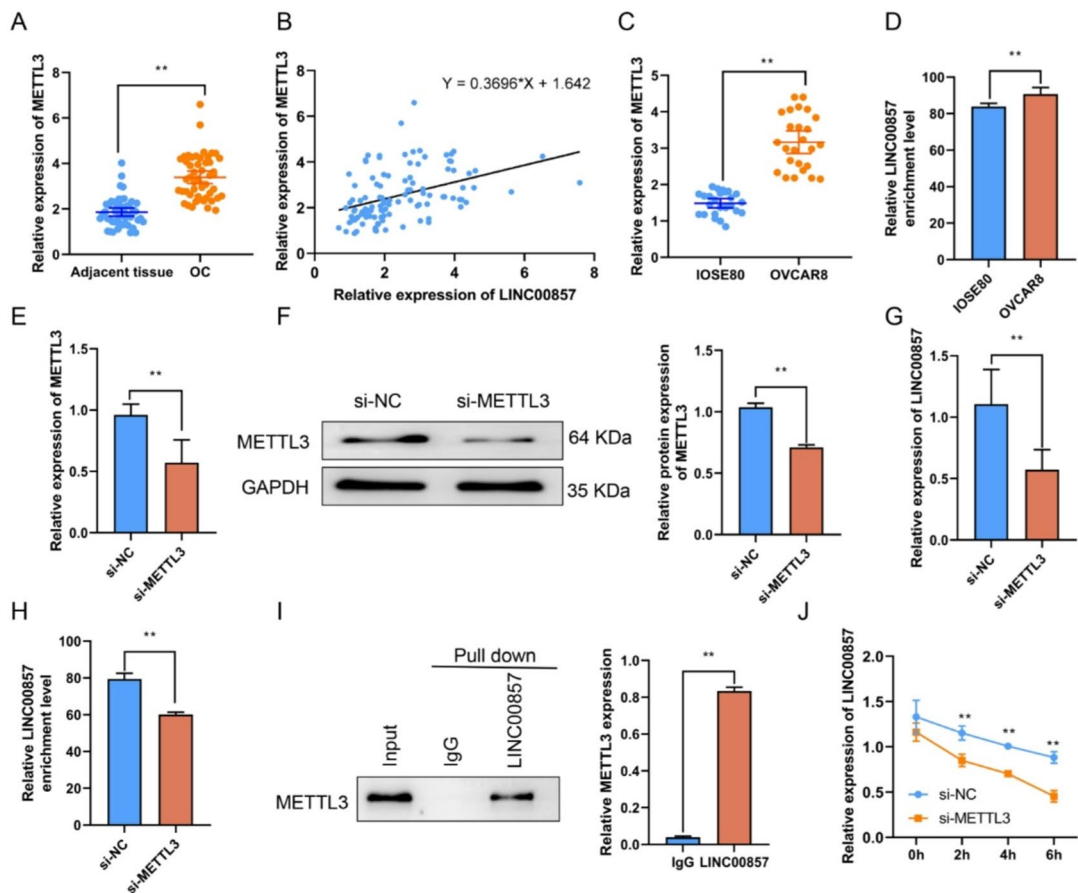


Fig. 4. METTL3 highly expresses in ovarian cancer cells and promotes the LINC00857 expression by m6A modification. (A) Relative expression levels of METTL3 in OC tissues compared to adjacent normal tissues using qRT-PCR ($n=50$). (B) The correlation between LINC00857 and METTL3 expression analyzed by Pearson ($n=108$). (C) Relative expression levels of METTL3 in OC cell line OVCAR8 compared to normal ovarian epithelial cell line IOSE80 using qRT-PCR ($n=25$). (D) The m6A enrichment levels of LINC00857 in IOSE80 and OVCAR8 cells were measured using the MeRIP-qPCR kit ($n=25$). (E) Relative METTL3 mRNA expression levels in OVCAR8 cells transfected with si-METTL3 or si-NC ($n=5$). (F) Western blot analysis showing METTL3 protein expression in OVCAR8 cells transfected with si-NC or si-METTL3 ($n=3$). (G) Relative mRNA expression of LINC00857 in OVCAR8 cells after METTL3 knockdown (si-METTL3) compared to the si-NC group ($n=5$). (H) m6A enrichment levels of LINC00857 in OVCAR8 cells transfected with si-METTL3 or si-NC using MeRIP-qPCR ($n=5$). (I) RNA pull-down assay showing the binding interaction between LINC00857 and METTL3 ($n=5$). (J) RNA stability assay indicating the relative expression of LINC00857 over time in OVCAR8 cells transfected with si-METTL3 or si-NC ($n=5$). Data were presented as mean \pm SD; ** $p < 0.01$; statistical significance was determined using unpaired Student's t-test. METTL3, methyltransferase-like 3; OC, ovarian cancer; m6A, N6-methyladenosine.

LINC00857 reverses the migration, invasion, proliferation, and stemness of OVCAR8 cells inhibited by METTL3 down-regulation

To determine the functional relevance of METTL3-mediated m6A modification of LINC00857 in OC progression, rescue experiments were performed by overexpressing LINC00857 in METTL3-knockdown OVCAR8 cells. Knockdown of METTL3 alone significantly reduced cell viability, invasion, migration, and sphere-forming capabilities, as demonstrated by CCK-8, Transwell, scratch, and sphere-formation assays ($p < 0.01$) (Fig. 5A–D). However, overexpression of LINC00857 in METTL3-knockdown cells partially rescued these effects, restoring cell viability, invasion, migration, and stemness.

Western blot analysis further confirmed that knockdown of METTL3 reduced the expression of stemness-related proteins, including NANOG, SOX2, and Oct4, while overexpression of LINC00857 reversed these effects ($p < 0.01$) (Fig. 5E–F). These findings suggested that METTL3 promoted OC progression by enhancing LINC00857 stability, which in turn drove cell proliferation, migration, invasion, and stemness.

LINC00857 reverses the effect of down-regulation of METTL3 on YAP1

Given the role of LINC00857 in activating the YAP1 pathway, we further investigated whether METTL3 influenced YAP1 signaling through LINC00857. Western blot analysis revealed that knockdown of METTL3

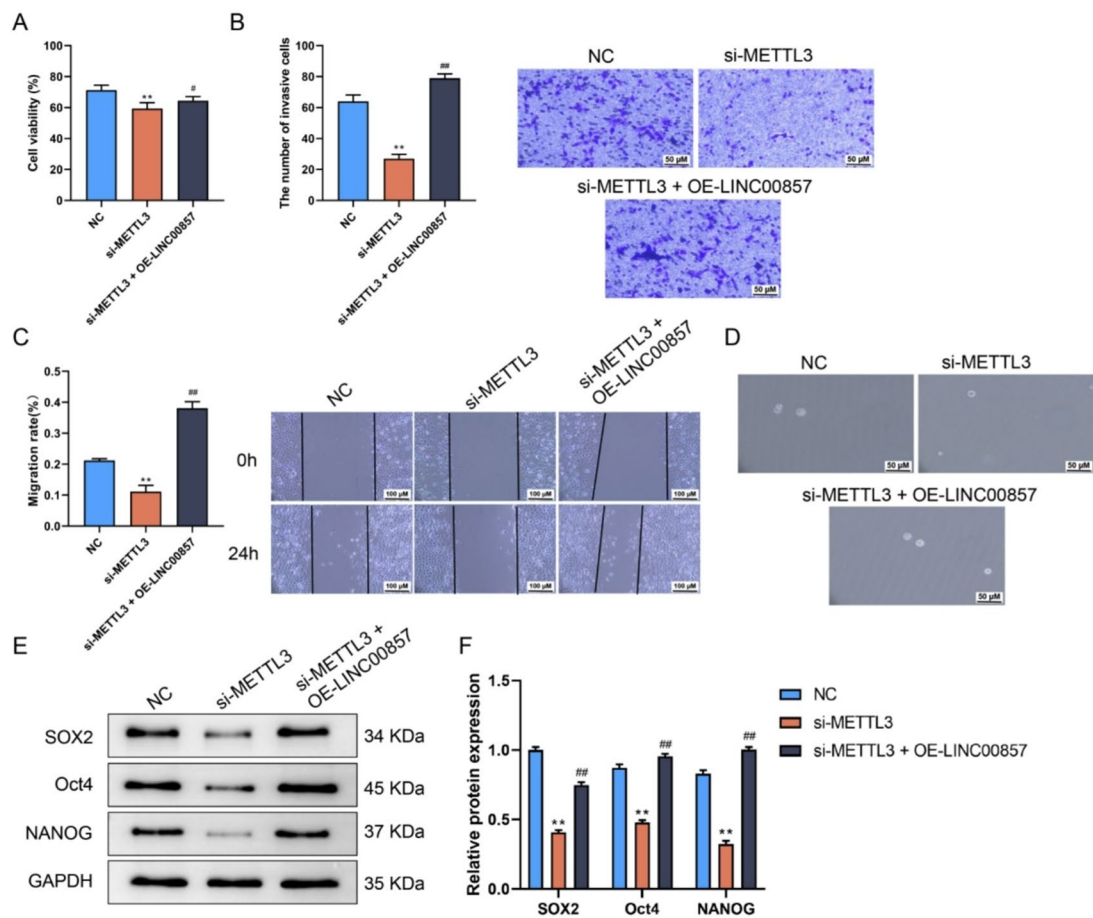


Fig. 5. LINC00857 reverses the migration, invasion, proliferation, and stemness of OVCAR8 cells inhibited by METTL3 down-regulation. **(A)** Cell viability of OVCAR8 cells was assessed using CCK-8 assay. **(B)** Cell invasion was evaluated using Transwell assay (scale bar = 50 μ m). **(C)** Cell migration was measured using scratch assay (scale bar = 100 μ m). **(D)** Representative images of sphere-formation assays showing the sphere-forming capability of OVCAR8 cells in each group (scale bar = 50 μ m). **(E-F)** Western blot analysis showing the protein levels of SOX2, Oct4, and NANOG in OVCAR8 cells. Data were presented as mean \pm SD ($n = 3 \sim 5$); ** $p < 0.01$ vs. NC; # $p < 0.01$ vs. si-METTL3; statistical analysis was performed using one-way ANOVA followed by Tukey's post hoc test. METTL3, methyltransferase-like 3; CCK-8, Cell Counting Kit-8; SOX2, SRY-box transcription factor 2; NANOG, Nanog homeobox; Oct4, octamer-binding transcription factor 4.

significantly decreased YAP1 and TEAD4 proteins levels, while increasing the levels of p-YAP1 and p-LATS1, indicating inactivation of the pathway. By contrast, overexpression of LINC00857 in METTL3-knockdown cells restored YAP1 and TEAD4 levels while reducing p-YAP1 and p-LATS1 levels ($p < 0.01$) (Fig. 6A-B). The results above demonstrated that METTL3 regulated YAP1 activation through LINC00857 stabilization, further linking METTL3-mediated m6A modification to OC progression.

Discussion

Despite continuous advancements in therapeutic strategies for OC, the survival rate and prognosis for OC patients remain unsatisfactory¹⁸. The primary reason is the insufficient understanding of the molecular mechanisms that contribute to the OC development and progression. The OC development is associated with alterations in gene expression, epigenetic modifications, and other complicated conditions¹⁹. These complex conditions emphasize the need for in-depth research to explain the molecule mechanisms of OC and to find appropriate treatment targets and biomarkers. Such efforts will contribute to establishing novel treatment methods and programs for OC and improving the prognosis and survival rate of patients with OC. Given that both METTL3 and YAP1 have been identified as drivers of therapeutic resistance and recurrence in ovarian cancer, elucidating the regulatory axis of METTL3-LINC00857-YAP/TEAD may provide novel molecular targets for overcoming resistance and improving patient survival.

LncRNAs are often observed to be abnormally expressed in cancers and play a significant role in the progression of malignant tumors, including OC. Of them, lncRNA TP73-AS1 has been demonstrated to be highly expressed in OC tumor tissues and associated with poor patient prognosis, whereas knocking down TP73-AS1 can inhibit the growth of in-vivo tumor²⁰. As demonstrated by Fang et al., the lncRNA HLA-F-AS1

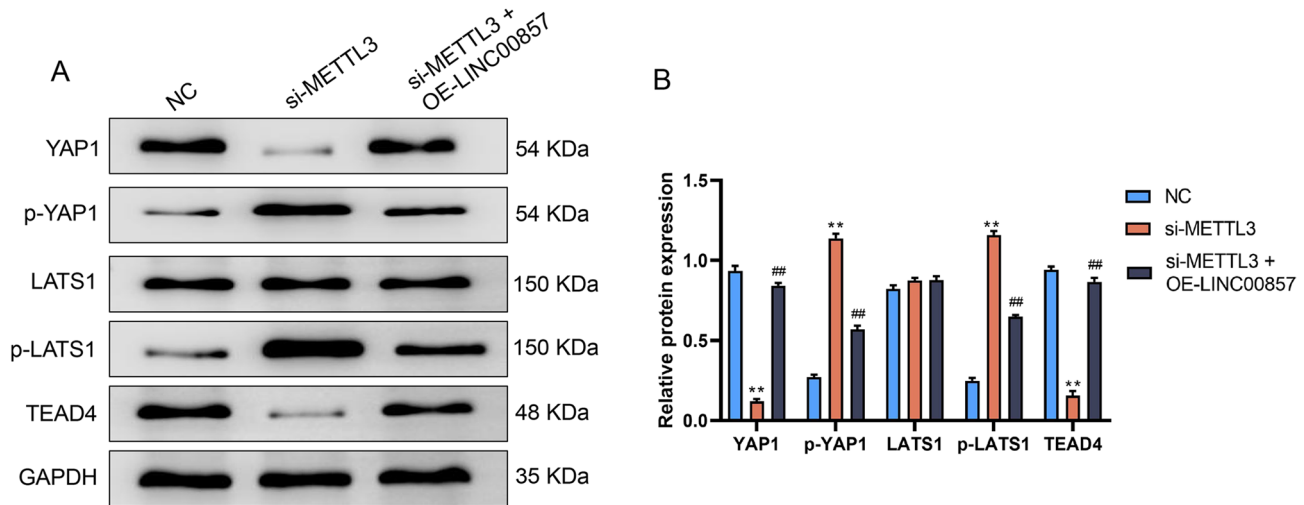


Fig. 6. LINC00857 reverses the effect of down-regulation of METTL3 on YAP1. (A) Representative protein bands of YAP1, p-YAP1, LATS1 and TEAD4 in OVCAR8 cells across groups. (B) Quantification of protein expression levels normalized to GAPDH. Data were presented as mean \pm SD ($n=3$); ** $p < 0.01$ vs. NC; # $p < 0.01$ vs. si-METTL3; statistical analysis was performed using one-way ANOVA followed by Tukey's post hoc test. METTL3, methyltransferase-like 3; YAP1, yes-associated protein 1; p-YAP1, phosphorylated-YAP1; LATS1, large tumor suppressor 1; TEAD4, TEA domain transcription factor 4.

expression in OC was remarkably down-regulated, but the progression of OC could be significantly inhibited after up-regulating lncRNA HLA-F-AS1²¹. In addition, lncRNA SNHG15 was up-regulated in OC, and an elevated lncRNA SNHG15 expression level was indicative of a poor prognosis of OC; lncRNA SNHG15 knockdown suppressed OC proliferation and promoted apoptosis²². Taken together, lncRNAs are key contributors to the OC progression. This study illustrated a notable up-regulation in the LINC00857 expression levels both in OC tissues and cells. Moreover, when knocking down the LINC00857 expression, the viability, invasion, and migration capability of cells all exhibited a significant decrease. However, when LINC00857 was overexpressed, the contrary phenomenon occurred. Our findings are consistent with those reported by Lin et al.¹⁰. Notably, we observed the correlation between LINC00857 and the stemness of OC cells. LncRNAs, such as lncRNA WDFY3-AS2²³, have been previously identified as crucial regulators of OC cell stemness. Stemness, in turn, is strongly correlated with the growth of tumors and the development of medicine resistance²⁴. Collectively, LINC00857 serves as a key signal molecule for maintaining the development of OC. Unlike previously reported lncRNAs in OC, our study is the first to demonstrate that LINC00857 is stabilized by METTL3-mediated m6A modification, thereby linking epitranscriptomic regulation to Hippo/YAP pathway activation.

YAP1, a highly efficient transcriptional activator, mainly acts on cell development, stemness maintenance, tissue homeostasis and regeneration. Nevertheless, p-YAP1 is translocated out of the nucleus, resulting in reduced transcriptional activity²⁵. Abnormal YAP1 expression is associated with cancer progression, invasion, and initiation, and its overexpression is widely regarded as a marker of poor prognosis²⁶. In addition, both TEAD and LATS are regulating molecules to maintain YAP1 pathway activity²⁷. Interestingly, the YAP1 pathway with high activity levels can be observed in many cancers, and this phenomenon may correlate with lncRNA regulation²⁸. LncRNA MLK7-AS1 has been reported to enhance the OC progression via activating the YAP1 pathway²⁹. Besides, lncRNA FLVCR1-AS1 facilitates the invasion, migration, progression, and epithelial-mesenchymal transition process of OC cells by activating the YAP1 pathway³⁰. LINC00857 has also been proved to facilitate the OC progression and glycolysis by activating the YAP1 pathway¹⁰. In this study, YAP1 had a considerably high expression in OC tissues. Additionally, we re-confirmed that LINC00857 knockdown would remarkably inhibit YAP1 pathway activity, whereas overexpression of LINC00857 significantly activated this pathway.

As the most prevalent modification of eukaryotic RNA, m6A is critical for physiological processes and cancer progression³¹. For instance, m6A is closely related to the stability of RNA. At present, 28 proteins related to m6A modification have been identified, among which METTL3 is the main methyltransferase responsible for triggering m6A modification of various types of RNA to enhance RNA stability³². Interestingly, the direct relationship between METTL3 and lncRNAs is often pivotal in cancer¹⁴. In clinical tissues collected in this study, a positive correlation was found in the METTL3 and LINC00857 expression levels, and both of them had significantly high expression in OC cells and tissues. Previous research discovered that METTL3 was commonly in a high expression state as a carcinogenic gene in cancers including liver cancer³³, breast cancer³⁴ and OC³⁵. After knocking down the METTL3 expression level in OC cells, a remarkable reduction was observed in the LINC00857 expression level, m6A modification level and stability. The binding between LINC00857 and METTL3 was further proved using the RNA pull-down assay. Notably, this study demonstrated that LINC00857 was modulated by METTL3-mediated m6A modification for the first time. Our findings provided a preliminary explanation for the up-regulation of LINC00857 expression observed in multiple cancers. Further, we knocked

down METTL3 and overexpressed LINC00857 in OVCAR8 cells. The viability, invasion, migration, and sphere-formation capability of OC cells were significantly inhibited after the knockdown of METTL3, whereas highly expressing LINC00857 reversed the effect of knocking down METTL3 alone. In addition, METTL3 can affect the activity of the YAP1 pathway by mediating multiple RNA modifications³⁶. The result from Chen et al.³⁷ uncovered that METTL3 promoted colorectal cancer metastasis by inducing m6A modification of circ1662 to accelerate the nuclear localization of YAP1. Xia et al.³⁸ revealed that METTL3 could induce lncRNA lnc-CTHCC by activating YAP1 transfection, resulting in hepatocellular carcinogenesis. Similarly, this study exhibited that after knocking down METTL3, the activity of the YAP1 pathway in cells was remarkably decreased. The fact that METTL3 could mediate m6A modification of LINC00857 to activate the YAP1 pathway was re-emphasized.

From a translational perspective, these findings are of potential clinical importance. Since aberrant activation of YAP1 signaling is associated with chemoresistance and recurrence in OC, the identification of the METTL3–LINC00857–YAP/TEAD axis provides a promising therapeutic avenue. Targeting this axis may sensitize ovarian cancer cells to platinum-based chemotherapy and improve patient outcomes, highlighting LINC00857 as both a biomarker and a potential therapeutic target.

Nevertheless, several limitations of this study should be acknowledged. First, the experiments were restricted to the cellular level, without extending the findings to animal models, which limits the translational impact. In future studies, we plan to employ xenograft and orthotopic tumor models to validate the role of LINC00857 and METTL3 in vivo. Second, although LINC00857 expression was validated in OVCAR8 and normal ovarian epithelial cells (IOSE80), additional normal and tumor cell lines should be included in subsequent research to confirm the generalizability of our findings. Third, all functional assays were performed in a single ovarian cancer cell line, where both knockdown and overexpression were conducted; an improved approach will be to knock down LINC00857 in cell lines with naturally high expression and to overexpress it in those with low expression levels. Fourth, the direct regulatory relationship between LINC00857 and YAP1 has not yet been elucidated, and experiments such as RIP or luciferase reporter assays are required to clarify whether the regulation is direct or mediated via upstream effectors. Fifth, although we confirmed METTL3-mediated m6A enrichment on LINC00857, we did not map the precise modification sites, which will be addressed in future work using m6A-seq and site-directed mutagenesis. Finally, the mechanisms underlying the abnormal expression of METTL3 in OC remain unexplored, and further investigation is needed.

Conclusion

In conclusion, this study demonstrated a notable increase in the expression levels of LINC00857 and METTL3 in OC tissues. Furthermore, METTL3-mediated m6A modification of LINC00857 contributed to the stability of LINC00857. In addition, LINC00857 could induce YAP1 pathway activation, thereby enhancing OC cell viability, migration, invasion, and stemness.

Data availability

The datasets used and/or analyzed during the current study are available from the corresponding author on reasonable request.

Received: 3 July 2025; Accepted: 16 October 2025

Published online: 20 November 2025

References

1. Lheureux, S., Braunstein, M. & Oza, A. M. Epithelial ovarian cancer: evolution of management in the era of precision medicine. *CA Cancer J. Clin.* **69** (4), 280–304 (2019).
2. Bray, F. et al. Global cancer statistics 2022: GLOBOCAN estimates of incidence and mortality worldwide for 36 cancers in 185 countries. *CA Cancer J. Clin.* **74** (3), 229–263 (2024).
3. Lheureux, S. et al. Epithelial ovarian cancer. *Lancet* **393** (10177), 1240–1253 (2019).
4. Meyer, L. A. et al. Neoadjuvant chemotherapy in elderly women with ovarian cancer: rates of use and effectiveness. *Gynecol. Oncol.* **150** (3), 451–459 (2018).
5. He, S. L. et al. LncRNA KCNQ1OT1 promotes the metastasis of ovarian cancer by increasing the methylation of EIF2B5 promoter. *Mol. Med.* **28** (1), 112 (2022).
6. Tan, Y. T. et al. LncRNA-mediated posttranslational modifications and reprogramming of energy metabolism in cancer. *Cancer Commun. (Lond.)* **41** (2), 109–120 (2021).
7. Ren, X. et al. Exploring the oncogenic roles of LINC00857 in pan-cancer. *Front. Pharmacol.* **13**, 996686 (2022).
8. Zhang, W. et al. Mutant p53 driven-LINC00857, a protein scaffold between FOXM1 and deubiquitinase OTUB1, promotes the metastasis of pancreatic cancer. *Cancer Lett.* **552**, 215976 (2023).
9. Pang, K. et al. Long non-coding RNA LINC00857 promotes gastric cancer cell proliferation and predicts poor patient survival. *Oncol. Lett.* **16** (2), 2119–2124 (2018).
10. Lin, X. et al. LncRNA LINC00857 regulates the progression and Glycolysis in ovarian cancer by modulating the Hippo signaling pathway. *Cancer Med.* **9** (21), 8122–8132 (2020).
11. Shen, C. et al. Long non-coding rnas: emerging regulators for chemo/immunotherapy resistance in cancer stem cells. *Cancer Lett.* **500**, 244–252 (2021).
12. Liu, J., Yuan, J. F. & Wang, Y. Z. METTL3-stabilized LncRNA SNHG7 accelerates Glycolysis in prostate cancer via SRSF1/c-Myc axis. *Exp. Cell. Res.* **416** (1), 113149 (2022).
13. Liu, H. T. et al. LncRNA THAP7-AS1, transcriptionally activated by SP1 and post-transcriptionally stabilized by METTL3-mediated m6A modification, exerts oncogenic properties by improving CUL4B entry into the nucleus. *Cell. Death Differ.* **29** (3), 627–641 (2022).
14. Song, Z. et al. LncRNA MALAT1 regulates METTL3-mediated PD-L1 expression and immune infiltrates in pancreatic cancer. *Front. Oncol.* **12**, 1004212 (2022).
15. Meng, X. et al. m(6)A-Mediated upregulation of LINC00857 promotes pancreatic cancer tumorigenesis by regulating the miR-150-5p/E2F3 axis. *Front. Oncol.* **11**, 629947 (2021).

16. Ma, L. & Zhang, Z. The contribution of databases towards Understanding the universe of long non-coding RNAs. *Nat. Rev. Mol. Cell. Biol.* **24** (9), 601–602 (2023).
17. Zhang, H. et al. m6A methyltransferase METTL3-induced LncRNA SNHG17 promotes lung adenocarcinoma gefitinib resistance by epigenetically repressing LATS2 expression. *Cell. Death Dis.* **13** (7), 657 (2022).
18. Zhao, Y. et al. LncRNA-MSC-AS1 inhibits the ovarian cancer progression by targeting miR-425-5. *J. Ovarian Res.* **14** (1), 109 (2021).
19. Miao, Y. et al. Prognostic significance of preoperative prognostic nutritional index in epithelial ovarian cancer patients treated with Platinum-Based chemotherapy. *Oncol. Res. Treat.* **39** (11), 712–719 (2016).
20. Wang, X. et al. The LncRNA TP73-AS1 promotes ovarian cancer cell proliferation and metastasis via modulation of MMP2 and MMP9. *J. Cell. Biochem.* **119** (9), 7790–7799 (2018).
21. Fang, W. & Xia, Y. LncRNA HLA-F-AS1 attenuates the ovarian cancer development by targeting miR-21-3p/PEG3 axis. *Anticancer Drugs.* **33** (7), 671–681 (2022).
22. Wang, Y. et al. LncRNA SNHG15 promotes ovarian cancer progression through regulated CDK6 via sponging miR-370-3 Biomed Res Int, 2021: 9394563. (2021).
23. Wu, Y. et al. LncRNA WDFY3-AS2 promotes cisplatin resistance and the cancer stem cell in ovarian cancer by regulating hsa-miR-139-5p/SDC4 axis. *Cancer Cell. Int.* **21** (1), 284 (2021).
24. Chen et al. Cancer stemness Meets immunity: from mechanism to therapy. *Cell. Rep.* **34** (1), 108597 (2021).
25. Collak, F. K. et al. Increased expression of YAP1 in prostate cancer correlates with extraprostatic extension. *Cancer Biol. Med.* **14** (4), 405–413 (2017).
26. Jin, Z. & Chen, B. LncRNA ZEB1-AS1 regulates colorectal cancer cells by MiR-205/YAP1 axis. *Open. Med. (Wars).* **15**, 175–184 (2020).
27. Szulzewsky, F., Holland, E. C. & Vasioukhin, V. YAP1 and its fusion proteins in cancer initiation, progression and therapeutic resistance. *Dev. Biol.* **475**, 205–221 (2021).
28. He, X. Y. et al. LncRNA modulates Hippo-YAP signaling to reprogram iron metabolism. *Nat. Commun.* **14** (1), 2253 (2023).
29. Yan, H. et al. Retraction Note: Long noncoding RNA MLK7-AS1 promotes ovarian cancer cells progression by modulating miR-375/YAP1 axis. *J. Exp. Clin. Cancer Res.* **39** (1), 233 (2020).
30. Yan, H. et al. LncRNA FLVCR1-AS1 mediates miR-513/YAP1 signaling to promote cell progression, migration, invasion and EMT process in ovarian cancer. *J. Exp. Clin. Cancer Res.* **38** (1), 356 (2019).
31. Peer, E., Rechavi, G. & Dominissini, D. Epitranscriptomics: regulation of mRNA metabolism through modifications. *Curr. Opin. Chem. Biol.* **41**, 93–98 (2017).
32. Hu, B. B. et al. N(6)-methyladenosine (m(6)A) RNA modification in Gastrointestinal tract cancers: roles, mechanisms, and applications. *Mol. Cancer.* **18** (1), 178 (2019).
33. Chen, M. et al. RNA N6-methyladenosine methyltransferase-like 3 promotes liver cancer progression through YTHDF2-dependent posttranscriptional Silencing of SOCS2. *Hepatology* **67** (6), 2254–2270 (2018).
34. Cai, X. et al. HBXIP-elevated methyltransferase METTL3 promotes the progression of breast cancer via inhibiting tumor suppressor let-7g. *Cancer Lett.* **415**, 11–19 (2018).
35. Bi, X. et al. METTL3 promotes the initiation and metastasis of ovarian cancer by inhibiting CCNG2 expression via promoting the maturation of pri-microRNA-1246. *Cell. Death Discov.* **7** (1), 237 (2021).
36. Ni, X. F. et al. The hepatic microenvironment promotes lung adenocarcinoma cell proliferation, metastasis, and epithelial-mesenchymal transition via METTL3-mediated N6-methyladenosine modification of YAP1. *Aging (Albany NY).* **13** (3), 4357–4369 (2021).
37. Chen, C. et al. N6-methyladenosine-induced circ1662 promotes metastasis of colorectal cancer by accelerating YAP1 nuclear localization. *Theranostics* **11** (9), 4298–4315 (2021).
38. Xia, A. et al. The cancer-testis LncRNA Lnc-CTHCC promotes hepatocellular carcinogenesis by binding HnRNP K and activating YAP1 transcription. *Nat. Cancer.* **3** (2), 203–218 (2022).

Author contributions

All authors contributed to the study conception and design. Material preparation, data collection and analysis were performed by Yiting Hong, Shengjun You, Ping Li, Yuchun Lv and Jinyang Zheng. The first draft of this manuscript was written by Xueke Lin and Pengming Sun and all authors commented on previous versions of the manuscript. All authors read and approved the final manuscript.

Funding

This research was supported by Quanzhou Science and Technology Plan Project, Fujian Province (Grant No. 2020N017s).

Declarations

Competing interests

The authors declare no competing interests.

Ethics approval and consent of participate

Prior to starting this study, the consent of the Ethics Committee of Quanzhou First Hospital Affiliated to Fujian Medical University was obtained, and all involved patients were informed and volunteered to participate. All patients involved provided informed consent and volunteered to take part in this study. The study was conducted in accordance with the Declaration of Helsinki.

Additional information

Supplementary Information The online version contains supplementary material available at <https://doi.org/10.1038/s41598-025-24958-w>.

Correspondence and requests for materials should be addressed to P.S.

Reprints and permissions information is available at www.nature.com/reprints.

Publisher's note Springer Nature remains neutral with regard to jurisdictional claims in published maps and institutional affiliations.

Open Access This article is licensed under a Creative Commons Attribution-NonCommercial-NoDerivatives 4.0 International License, which permits any non-commercial use, sharing, distribution and reproduction in any medium or format, as long as you give appropriate credit to the original author(s) and the source, provide a link to the Creative Commons licence, and indicate if you modified the licensed material. You do not have permission under this licence to share adapted material derived from this article or parts of it. The images or other third party material in this article are included in the article's Creative Commons licence, unless indicated otherwise in a credit line to the material. If material is not included in the article's Creative Commons licence and your intended use is not permitted by statutory regulation or exceeds the permitted use, you will need to obtain permission directly from the copyright holder. To view a copy of this licence, visit <http://creativecommons.org/licenses/by-nc-nd/4.0/>.

© The Author(s) 2025